

SIMULTANEOUS MODELLING OF ROCK FREEZING AND WATER
SEEPAGE AND ITS PRACTICAL APPLICATIONS

Zsolt Kesserű, L. Dusza, A. Widder and Cs. Kiss Máté
Central Institute for Mining Development
H-1037 Budapest, Mikoviny 2-4,
Hungary

ABSTRACT

All existing models of the rock freezing process are able to simulate the conductive heat transfer, but, however the convective terms are dominant in many cases, when water seepage also occurs. The origin of the majority of failures were caused by the effect of water seepage.

A new integrated finite difference simulation technique has been developed to model rock freezing and water seepage simultaneously. The mathematical model, the base of numerical algorithm, the input and output data, the verification of the model using analytical solutions and a rather sophisticated practical case history are discussed in the paper. Finally, the first practical application of the model to support decisions on the proper system of freezing and on the proper combination with depressurization of water bearing layers is presented as well.

1. PROBLEM PRESENTATION

During the past hundred years rock freezing operations have been successfully applied in the civil engineering and mining practice all over the world (Belferman 1982; Hegelman 1982; Ries 1982; Sabela 1982; Seleznev and Sedin 1982; Wild and Forrest 1984). Many difficulties and accidents also occurred mostly due to the effect of water seepage and/or thermal anomalies of sources (Honvéd 1986; Wild and Forrest 1984).

In many special cases a proper combination of drainage and rock freezing may also provide a better and/or cheaper solution (Seleznev and Sedin 1982), but nobody tries to use these combinations because of the unpredictable effects of water movement on the rock freezing process.

In order to size the rock freezing operations under high waterflow rates and to select and to design proper combinations of rock freezing and drainage

a computer simulation technique has been developed for simultaneous modelling of water seepage and rock freezing.

This paper presents briefly:

the mathematical model,
the computation,
the model verifications, and
the first practical applications.

2. THE MATHEMATICAL MODEL

The natural process of rock freezing under conditions of water seepage is characterized by the following balance equations referring to a small part of the space, dV , which has a boundary surface dA , in a small time interval, dt .

The mass balance:

$$\frac{d}{dt} \int_V \frac{p_w}{g} s_{rw} dV + \int_A p_w \vec{v}_w dA - \int_V q_{wi} = 0$$

where p_w is the water pressure

g is the gravitational acceleration

v_w is the water seepage rate

q_{wi} are water source terms

s_{rw} is the storage parameter of the rock-water system

for confined systems:

$$s_w = \Phi \cdot \beta_w \cdot g \cdot C_{rw}$$

for unconfined systems:

$$s_w = \Phi/h$$

where Φ is the rock-porosity

C_{rw} is the compressibility of rock-water system

β_w is the density of water (in function of temperature and water pressure)

h is the height of the water in the reservoir layer

The simplified impulse balance equation is given by the Carcy vector-equation.

$$\vec{v}_w = \frac{k}{\mu(T)} \cdot (\vec{v}_{p_w} - \beta_w \cdot g_{(p,T)})$$

where k is the permeability of rock

$\mu(T)$ is the dynamic viscosity of water depending on temperature, T

The energy balance is given by the equation of convective and conductive heat balance, taking into account the energy transport of phase transition.

$$\frac{d}{dt} \int_V [\Phi \cdot \rho_w C_w - (1 - \Phi) \rho_r C_r] T dV - \int_A K_{rw} \vec{V} \cdot \vec{n} dA + \int_A \rho_w C_w \vec{V} \cdot \vec{n} dA - \int_V (G_h + \rho_w \Phi G_{ft}) dV$$

where C_w and C_r is the specific heat storage capacity of water (w) and rock (r)

K_{rw} is the head conductivity of the rock-water system

G_h represents any extra head sources, eg freezing

$\pm G_{ft}$ in the specific head of water-ice phase transition (freezing or thawing)

3. COMPUTATION

3.1 The numerical model for computation

For the purpose of computation the space is represented by a structure of elements. Each element has its given geometry and physical parameters.

The basic balance equations are given as finite difference equations regarding the mass and heat transfer between each neighbour elements (eg between nodes n and m) during a given period Δt_i .

The mass-transfer equation including the Darcy's law is formed as follows:

$$\left(\frac{\rho_{rw} V_i}{g} \right) \frac{\Delta p_w}{\Delta t_i} = \left(\frac{K \rho A}{\mu} \right)_{ij} \frac{p_m - p_{in}}{D_{N,m} + D_{M,N}} - \left(\frac{K \rho^2 A}{\mu} \right)_{N,m} \cdot g + (G_f V_i)_N$$

The heat transfer

$$(\rho C)_M V_N \frac{\Delta T_N}{\Delta t} = \frac{(K_h A)_{N,m}}{D_{N,m} + D_{M,N}} (T_M - T_N) + \left(\frac{\rho C_F A K}{\mu} \right) (T_{N,M} - T_N) \left(\frac{p_m - p_n}{D_{N,M} + D_{M,N}} - 299 \right) + (G_h V)_N + (\rho \Phi G_{ft})_N$$

where indices N and M refer to the nodes (elements) N and M; the index NM refers to the interface of the two elements

D is the distance between the node and interface

η is the cosine of the angle of \vec{D} and the normal vector of the interface

S, μ are temperature dependent parameters in the mass transfer equation

At the same time there are parameters in the heat transfer equations which are influenced by the mass transfer, et $p_{wn} - p_{wm}$. It means that an interactive process is necessary to model the interactions between the heat and the mass transfer.

For the iterative solution of the above equations an integrated finite difference method is used.

3.2 Some details of computation

(i) Node network

A two or three dimensional network can be used. There is no limitation regarding the forms and volume of each element and the number of connections of each node. Each node is specified geometrically by their own parameters.

To cut the time and costs of network forming some standardized two or three dimensional network patterns are available. These standardized networks can be fitted to a given task using a multiplying factor.

For special purposes individual two or three dimensional networks can also be used.

(ii) Internal input parameters

The parameters of water are given in function of T and p

$$S_w(T, p) = a_1 T + a_2 T^2 + a_3 p_w + a_4 p_w^2 + a_5$$

where a_1, a_2, a_3, a_4, a_5 are input parameters

$\mu(T)$ is given by polynomes of given T_1, T_2, T_3, T_4 values

The initial water head or bottom-hole water pressure should be specified for each node.

The thermal parameters of water are:

C_w specific heat storage
 K_w heat conductivity
 $\pm G_{ft}$ ice-water phase transition heat

The parameters of rocks are given for rock types. 80-100 different rock types should be specified for each practical task.

Each rock type is specified by the following parameters:

No code number of rock type
 k permeability (water pressure dependent parameter)
 ρ_r density
 s_r storage
 Φ porosity
 C_r heat storage capacity
 K_r head conductivity

The same parameters should be specified for a frozen rock-water system, which is regarded as a "rock type" of another kind.

For each rock, a regional anisotropy type, and for each node-connection a local anisotropy, can also be modelled.

(iii) Boundary conditions

Almost all types of boundary conditions are available. These are:

- constant pressure nodes $(p)_b = \text{const}$
- time dependent pressure nodes (changing by time steps)

$$(p_b) t_1 - t_2 = C_1$$

$$(p_b) t_2 - t_3 = C_2$$

$$(p_b) t_3 - t_4 = C_3$$

- constant temperature nodes $(T)_b = \text{const}$ or time dependent temperature nodes

$$(T_b) t_1 - t_2 = C_1$$

$$(T_b) t_2 - t_3 = C_2$$

$$(T_b) t_3 - t_4 = C_3$$

- constant water recharge or drainage, or changing the same by time steps
 $q = \text{const}$

$$qt_1 - t_2 = C_1; qt_2 - t_3 = C_2; qt_3 - t_4 = C_3$$

- constant heat extraction/injection, as well as the same by time steps

$$G_i = \text{const}$$

- time dependent heat extraction/injection

$$Gt_1 - t_2 = C_1; Gt_2 - t_3 = C_2; Gt_3 - t_4 = C_3$$

- temperature dependent heat extraction/injection can be modelled for each node and for each time step by using function

$$G = A(t) \cdot T$$

where constants A can be changed in each time step

Using the special nodes listed above each kind of drainage and freezing can be easily computed.

Parameters for iteration should be specified also on the input list according to the feature of the process to be modelled. The computation can be stopped and restarted (restart option).

(iv) The output parameters

The output list provides all of the necessary information for design and for process control. The most important ones are as follows:

- water head,
- bottom-hole pressure, total water pressure difference for each node in all specified time steps,
- temperature and total temperatures changing for each node in all specified time steps,
- water balance and heat transport terms for each connection in the last time step,
- stored heat and mass for each rock type,
- mass and heat transfer along the boundaries.

The output data can also be plotted in the form of curves depending on the printing and plotting facilities of the users.

The first version of the program ran on Honeywell Bull 60/20 and IBM 370 computers. Now a new program-version is already available for a professional personal computer type IBM-AT.

Consequently the model can also be applied by the rock-freezing contractor firms themselves.

4. MODEL VERIFICATION

4.1 Comparison to analytical solutions

Analytical equations for describing the interaction of rock freezing and water seepage are not available. Consequently the computer model could be compared only with the analytical solution of rock freezing under conditions of one dimensional conductive heat transport which is given by the following equation according to Carslaw and Jager:

$$\frac{\partial T_1}{\partial t} = K_1 \Delta T_1 + Q \text{ and } \frac{\partial T_1}{\partial t} = K_2 \Delta T_2$$

where Q is the heat extraction and T_1 and T_2 are temperatures in the frozen phase and in the liquid phase. At the boundary of the frozen area $T_1 = T_2 = 0$ and

$$\frac{\partial T_1}{\partial x} K_2 - \frac{\partial T_2}{\partial x} = G_{ft} \frac{\partial R}{\partial t}$$

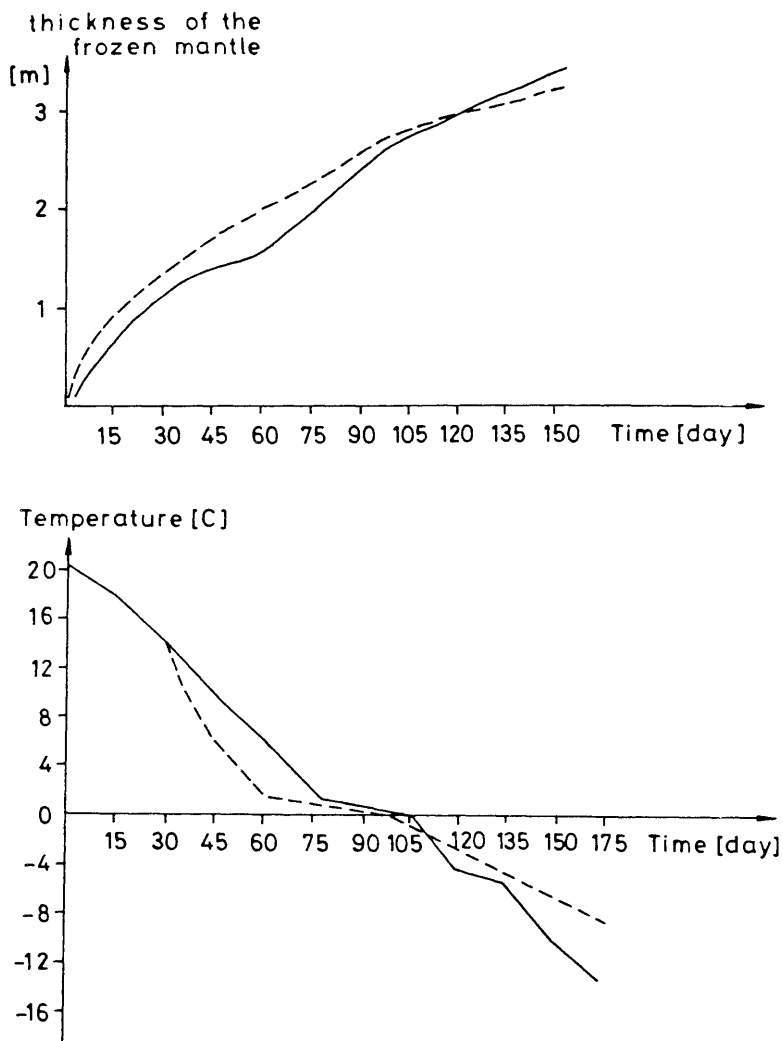


Figure 1 The temperature of a node under conditions of one-dimensional conductive heat transfer

Curve a analytical solution
Curve b numerical simulation

where R is the distance between the border of the two phases.

The result of the comparison is presented in Figure 1 where the progression of the boundary of the frozen mantle can be seen (see curves a and b). Although a few numbers of nodes were used, the fit of the computed curve (curve b) is quite acceptable.

4.2 Modelling of a "past-case"

For testing the ability of the model and for comparing the model outputs with the experiences, a "past case example" so-called "test case" was computed by our new simulation model.

(i) Brief history of the "test case"

3 years prior to completing this new simulation model a shaft was sunk under the protection of rock freezing through water bearing sands. Because of the high water seepage rate water inflow occurred and additional measures were also taken as described hereinafter. (For more details see Reference No 4.)

Figure 2 shows the schematized geological profile at the axis of the shaft. Although a relatively high flow rate (1.8 m/day) was estimated according to the regional hydrogeological feature, no local flow rate test was carried out before freezing.

The location of the temperature measuring holes (test holes) was not an appropriate either (see Figure 2). As a consequence of these preconditions, after a three months period of the intensive freezing, a quite good result was recorded in the temperature test holes in all of three water bearing layers. For this reason the shaft sinking operation started and continued through the first layer and approached the second (gravel) layer (see Figure 2) where the water inflow occurred, which increased to 3 m³/min. The differences between the output and input temperatures of the freezing fluid of each hole detected the location of the window of the frozen wall. This location, of course, was at the "streamside" zone of the frozen mantle. In order to stop the enlarging of the "window" on the frozen mantle the shaft was flooded.

A posterior water seepage rate and direction measurement in four test holes was conducted just upon the failure, which detected a much higher water flow rate (4 m/d) than estimated before. Of course, the direction of the flow was also in strong coincidence with the location of the window.

A grouting operation to close the "window" and additional freezing holes was decided and performed. After these measures the sinking operation was completed successfully. The time schedule of this case history is presented in Figure 2.

From the viewpoint of our model verification this past case history (freezing - water inflow - grouting, additional freezing and thawing) was quite a good "test case" to check almost all potentialities of the model and to compare the outputs of modelling with some data measured at the test case.

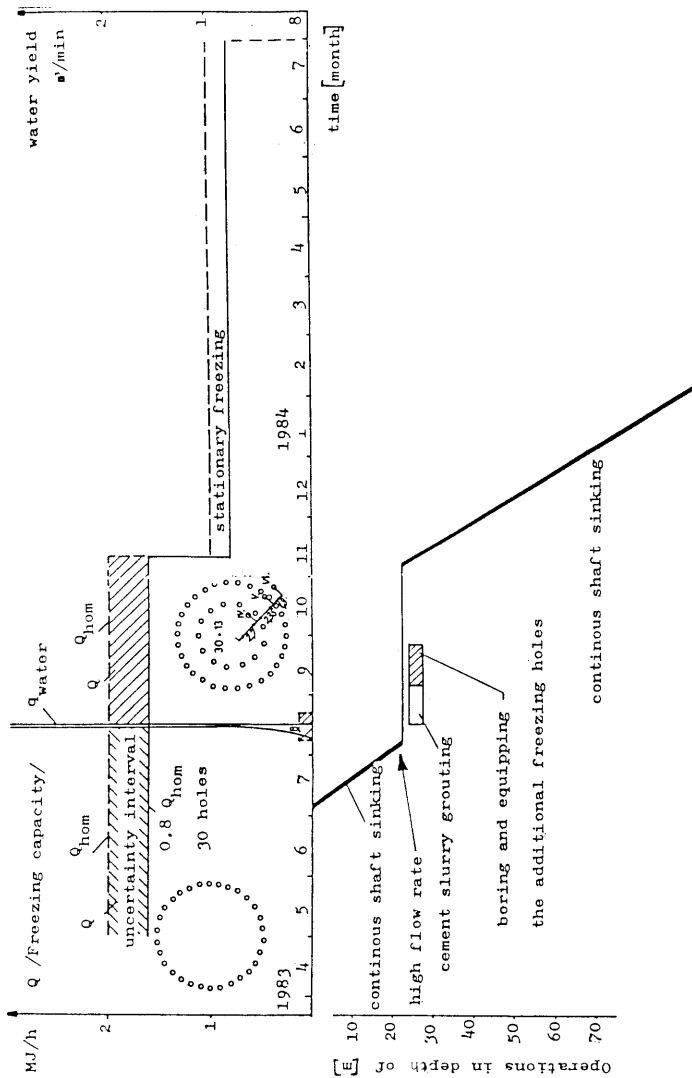
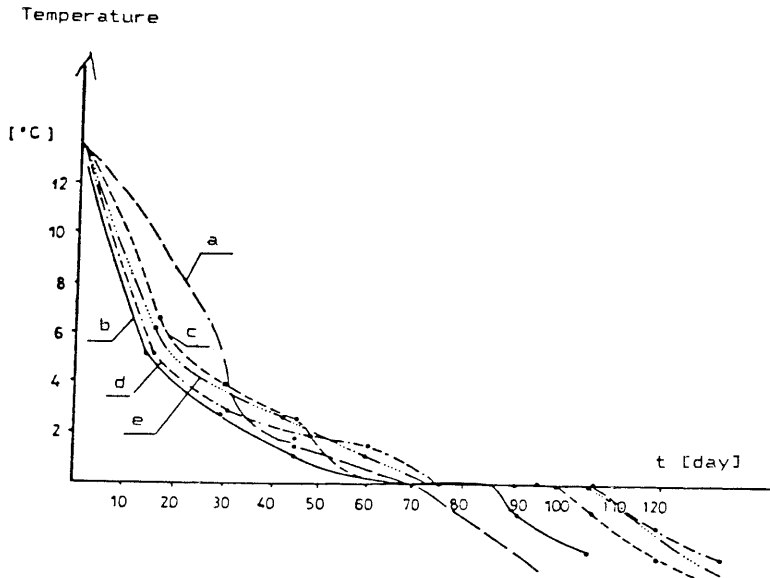


Figure 2 Time scheduling of the freezing, shaft sinking and other additional operations at the test case

(ii) Results of the model verification

For testing the working potentiality of the model the whole case history was modelled in a spherical three-layer model. The vertical and horizontal view of the node network can be seen in Figure 4. The direction of flow serves as a quasi-symmetry axis. For that reason only the half of the total space was modelled.



Actual and computed temperature in the test hole

- Curve a - - - measured
- Curve b - · - · - computed with original input data
- Curve c - - - - computed with increased supposed rate ($v = 5.2$ m/day)
- Curve d - · - · - computed with increased porosity
- Curve e ——— computed with $v=0$

Figure 3

The feature of the process and the key phenomena were compared for model verification.

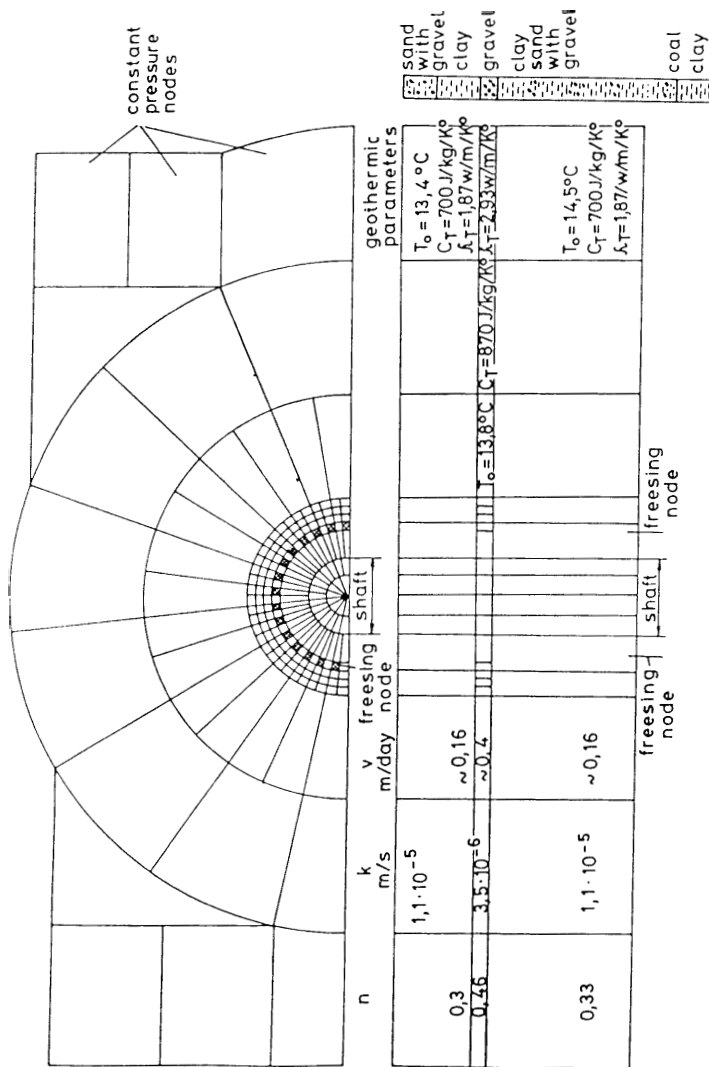


Figure 4 Vertical and horizontal view of node network for the "test case" (with parameters)

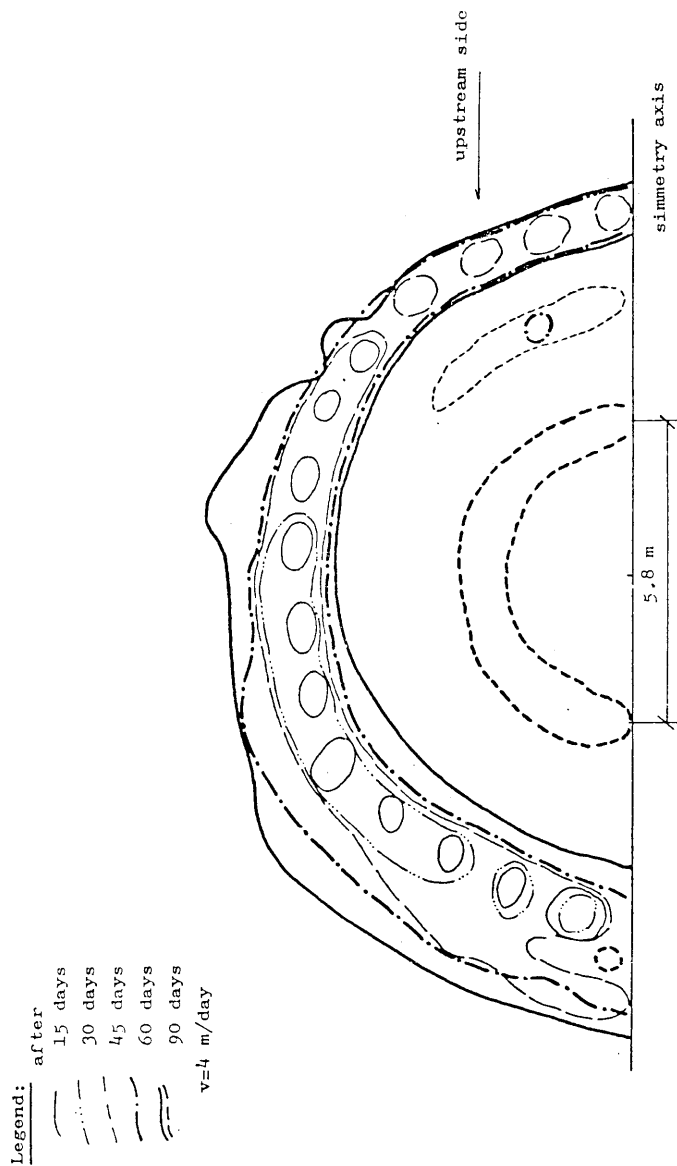


Figure 5 Steps of forming the frozen wall in the "gravellayer" during the first three months period of the test case

In the first phase of the freezing the detected temperature in the freezing hole and the presence and location of a window in the frozen wall provided bases for comparison.

Figure 3 shows the computed and measured temperatures in temperature test hole No 2. The computed curve b using the original input data according to Figure 4 shows quite a good general fit although there are controversial difference below and above 0°C.

The reason for these controversial differences was the insufficiency of the input data. Although the model is suitable to compute different freezing fluid temperatures for different time intervals, only an average freezing fluid temperature (-20°C) was used as the input for computation. It only appeared later that actually the freezing started with -13°C and was finished with -28°C.

Figure 5 shows different phases of forming the frozen wall and the water seepage. The last phase after 90 days shows a dangerously small wall thickness exactly in the area where the window was detected in the actual case.

The same Figure shows also the importance of the convective asymmetry term of the heat transfer (the asymmetry of forming the frozen wall) and the reason why the temperature-test hole, located improperly, showed a safety frozen mantle, although the streamside mantle was thin.

The enlarging of the window under the effect of the flowing water was modelled in the next step.

Figure 6 presents the computed temperature field and the status of the frozen mantle in the gravel layer just before stopping the water inflow. The process of enlarging the window can be seen in this Figure.

Then the effect of grouting was also modelled as a change of the permeability parameter (ie changing the code of the rock material) in the ground area. The modelling of the next freezing step by the use of additional holes shows the forming of a frozen area in the whole cross section of the shaft (see Figure 7). The same was detected during shaft sinking, but no temperature data were available for more sophisticated comparison.

Finally the thawing process was modelled, although no temperature data of that period were available; only the date of the first water inflow through the concrete wall of the shaft was known as a sign of forming the first window in the frozen mantle. The model results show that the window had been formed earlier than happened really. The reason for the difference may be the protective effect of the grouted zone, which isolated the water stream from the streamside area of the frozen mantle.

Some results of the thawing process is presented in Figure 8. Figure 8 (a) shows the temperature profiles of all three layers. The effect of the high flow rate is proved to be strong.

(iii) Parameter sensitivity analysis

The uncertainties of the input parameters were also tested using more values of the same input parameters for computation. Although more

Legend

- barrier of the frozen mantle
- - - line of 0°C
- · - · - the outer diameter of the shaft
- $v = 5,6 \text{ m/day}$

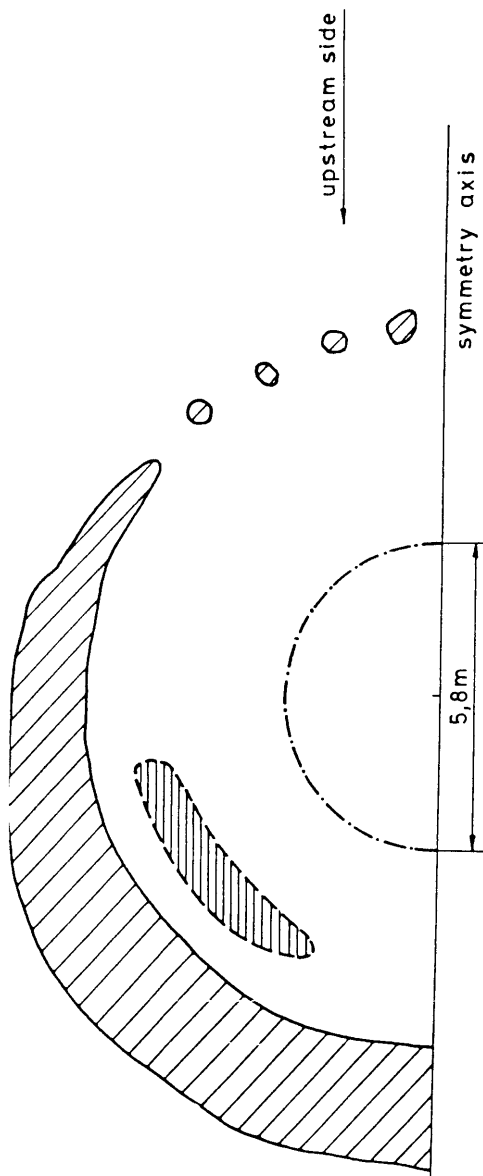


Figure 6 The computed temperature and the status of the frozen mantle at the test case just before stopping the water inflow

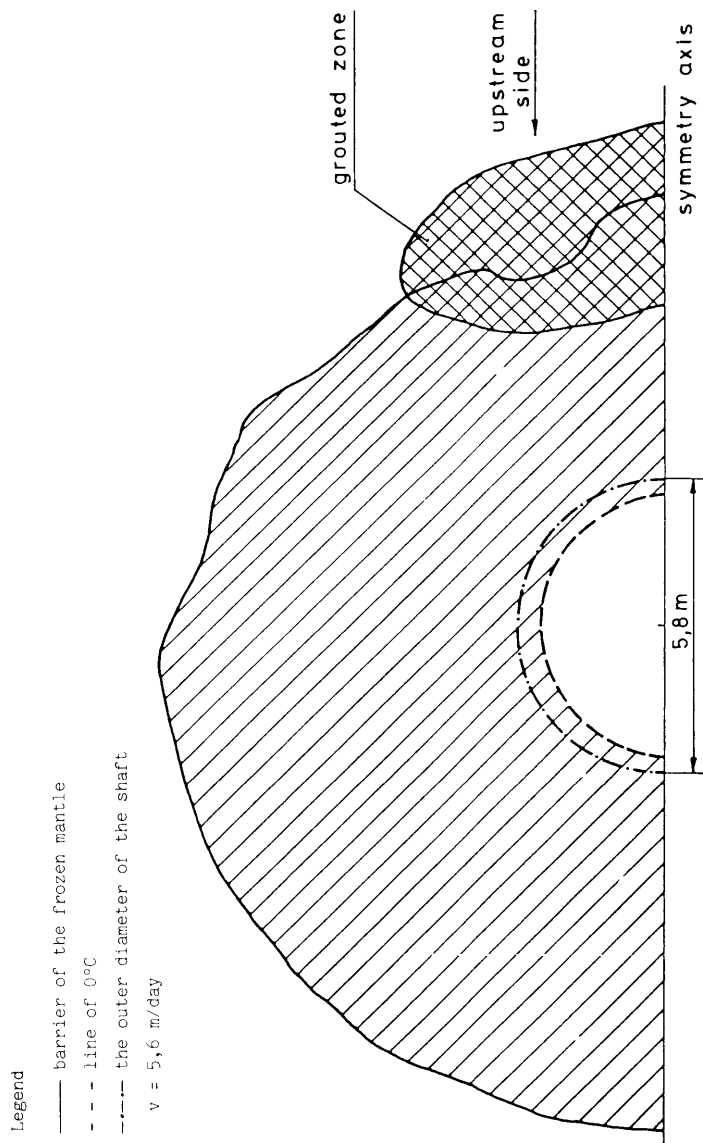


Figure 7 The status of the frozen mantle after grouting and using additional freezing holes

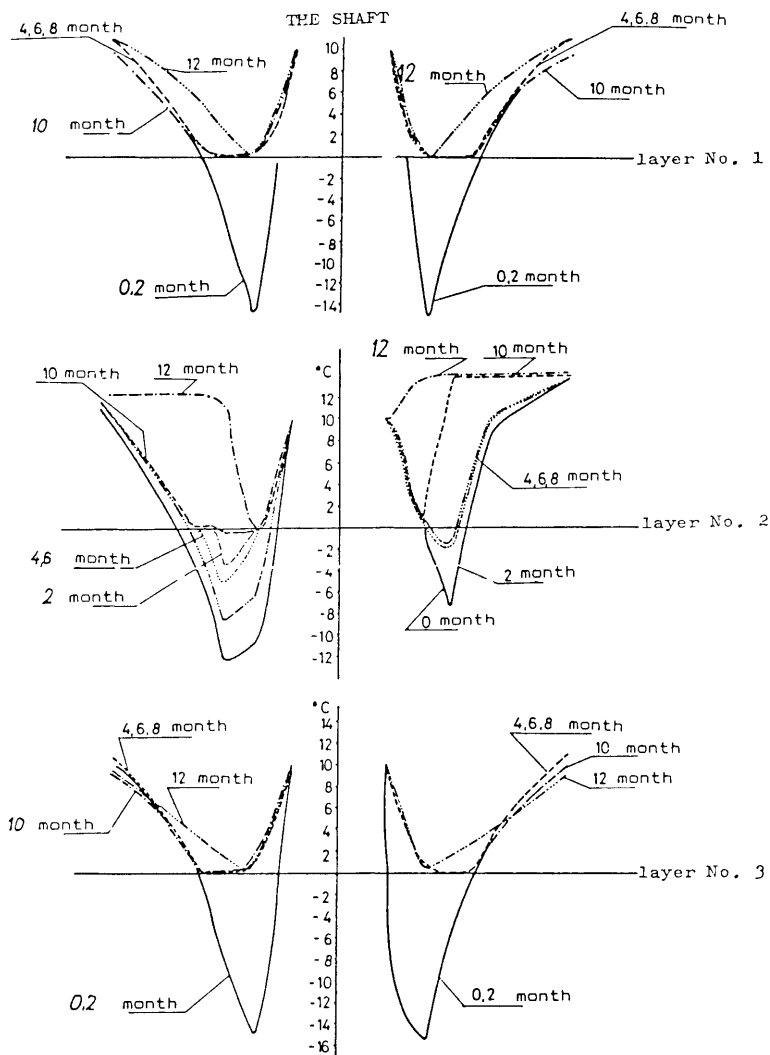


Figure 8 The thawing process of the test case
(a) Temperature profiles in all of the three layers

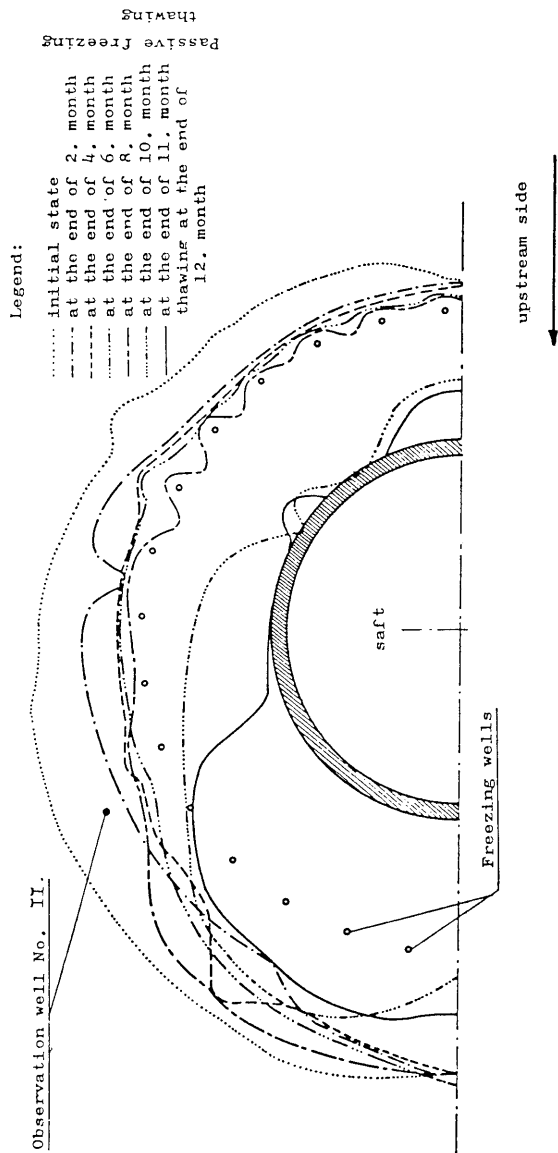


Figure 8 (b) The thawing process of the test case. The changing of the frozen mantle in the gravel layer

detailed investigations were carried on, only the most important consequences are mentioned hereinafter:

- The porosity (Φ) is one of the dominating factor (see curves b and c in Figure 3.
- Under conditions of water seepage the flow rate is the most dominating factor of the freezing process as demonstrated in Figure 6 where thermal cross sections parallel with the flow directions and at different flow rates can be seen.
But this strong impact of the water flow rate cannot be detected by the test holes located improperly (see Figure 3, curves b, c and e).
- The spherical three dimensional structure of the node network allows us to compare the vertical and horizontal terms of heat transport in Table 1. Although the "critical" gravel layer was surrounded by fine sand, where the flow rate was different by orders of magnitude, the vertical component of the heat transfer is practically negligible compared with the horizontal ones.

(iv) Some consequences of the verification and sensitivity analysis

- The potentiality of our new model was successfully demonstrated by modelling an extremely sophisticated practical case history.
- The key phenomena produced by the simulation fits quite well to the empirical ones and the numerical fit was also acceptable.
- The key input parameters to be determined most carefully are the porosity and the flow rate.
- It seems that for the majority of practical cases a two-dimensional network of nodes can also be applied (see Table 1), but a more detailed node network is necessary to provide data for supporting practical decisions for the purpose of design and managing.

Table 1 The comparison of the vertical and horizontal terms of the heat transfer in some important nodes of the medium/gravel/layer

Code number of nodes	The total heat transfer in the period of "active" freezing	
	In horizontal directions (four connections)	In vertical directions (one connection)
3	$+2.4 \cdot 10^9$	$-7 \cdot 10^9$
	$-29 \cdot 10^{10}$	
	$+28 \cdot 10^{10}$	
	$-6 \cdot 10^9$	
	$-2 \cdot 10^9$	
102	$.1 \cdot 10^{10}$	$-6.9 \cdot 10^8$
	$.2 \cdot 10^{10}$	
	$.6 \cdot 10^{10}$	

202	-6.10 ¹⁰	-58 10 ⁹
	.9.10 ¹⁰	
	.4.10 ¹⁰	
	-7.10 ¹⁰	

(v) A posteriori study to select the proper solution

The model study detected the main source of the failure: the high flow rate at the medium (gravel) water bearing layer. The dangerous impact of the water flow was not detected by the temperature test holes because of their improper location.

For testing the model potentiality we tried to select an "a posteriori" proper location of the freezing and temperature test holes under the given flow rate conditions of the past "test case".

An additional series of freezing holes (3 holes for half of the space) at the streamside area was applied in the model, and the total freezing capacity was distributed for all freezing holes. As presented in Figure 9 the effect of the additional holes almost eliminated the dangerous effect of the high water flow rate without any increase of the necessary freezing capacity. In this respect it should be noted that in our "test case" the high flow rate occurred only in one layer of small thickness. Consequently for other conditions the high flow rate may also require an increasing capacity of the freezing plant.

The proper location of the temperature test holes for the given conditions can be determined according to Figure 5. It deviates by 30-40° from the direction of the flow (at the streamside). Note: In other cases, other factors, eg the inclination of freezing holes, may also be determinative factors for locating temperature test holes.

5. PRACTICAL APPLICATIONS

5.1 The case

At Lyuko Colliery of the Borsod Coal Basin in North Hungary a new ventilation shaft with a depth of 260 m was planned.

The geological profile can be seen in Figure 10. Because of many soft, loose, water bearing layers, rock freezing was offered by the contractor. 19 freezing holes were planned in one circle, and two or three temperature test holes. The nominal capacity of the freezing plant was 1.7 MJ/h = 400,000 Kcal/h. Because of the limited capacity of the freezing plant, the freezing operation was planned to carry on in two steps; 0-125 m and 125-250 m.

The water flow conditions are not known completely. The water bearing layers between coal seams 3 and 4 are impacted by the mine drainage activity. The estimated hydraulic gradient is 0.1 m/m (direction SE-NW).

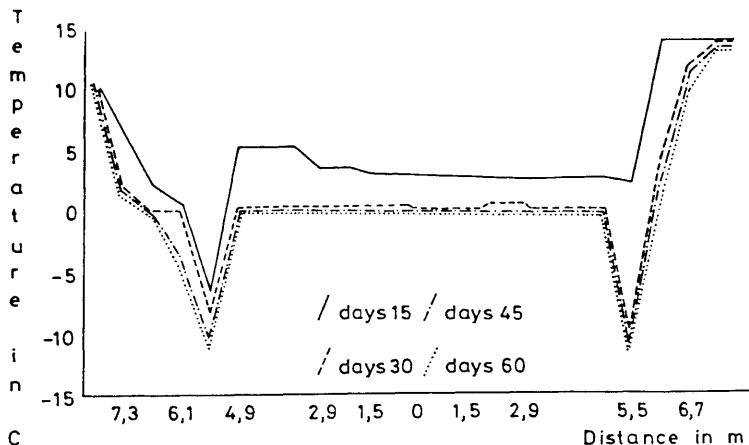


Figure 9 Temperature profile in the gravel layer at the "test case" using six additional holes at the streamside area (a posteriori variant)

The upper water bearing layers are under natural conditions, where the basis of erosion is south of this site. Consequently the supposed flow direction is N-S. A pleistocenic gravel layer was also detected at a shallow depth and a group of test holes was planned in order to determine the flow rate and direction. Because of the water flows and the low capacity of the freezing plant the Investor (Borsod Coal Mines) also considered combining rock freezing with the depressurization of the water bearing sands for the sake of minimizing the consequences of a "window" in the frozen mantle.

5.2 The tasks of the simulation model studies

The Investor asked our Institute to support his decisions by the use of simulation model studies even in the preliminary phase of the design work and during the operative management of the rock freezing as well.

The tasks were as follows:

For preliminary design

- Make comparison between freezing in one step and freezing in two steps.
- Study the effect of the inclination of holes with the purpose of determining the requirements for the drilling operation.

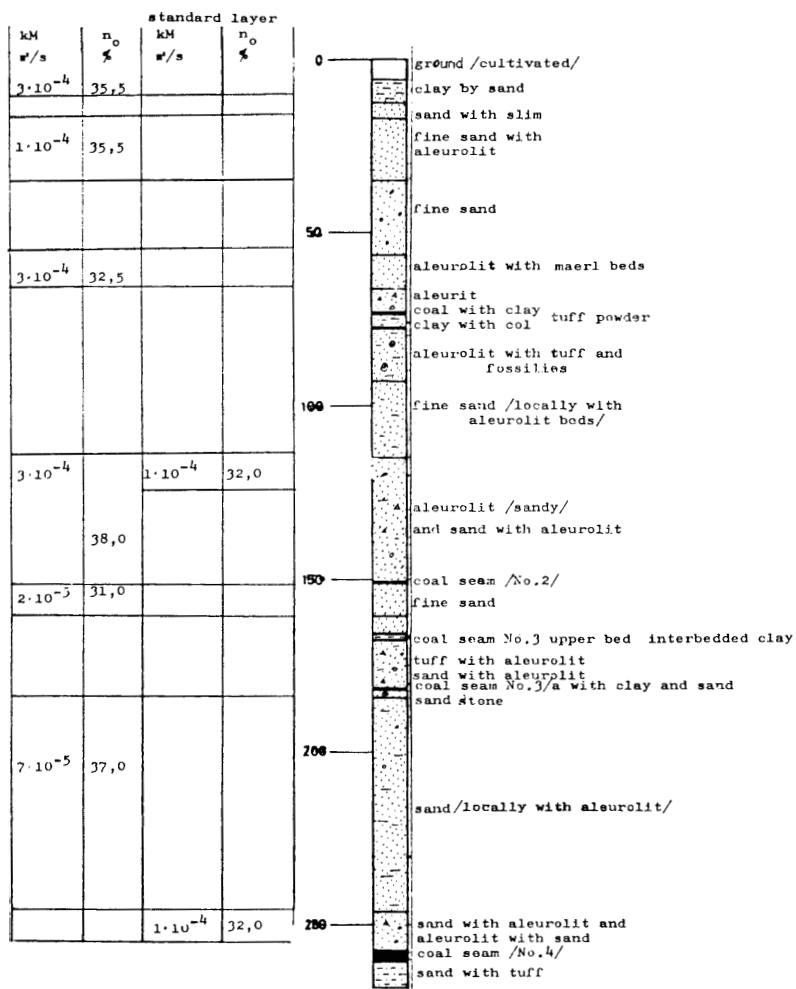


Figure 10 Geological profile of ventilation shaft planned at Lyuko Colliery

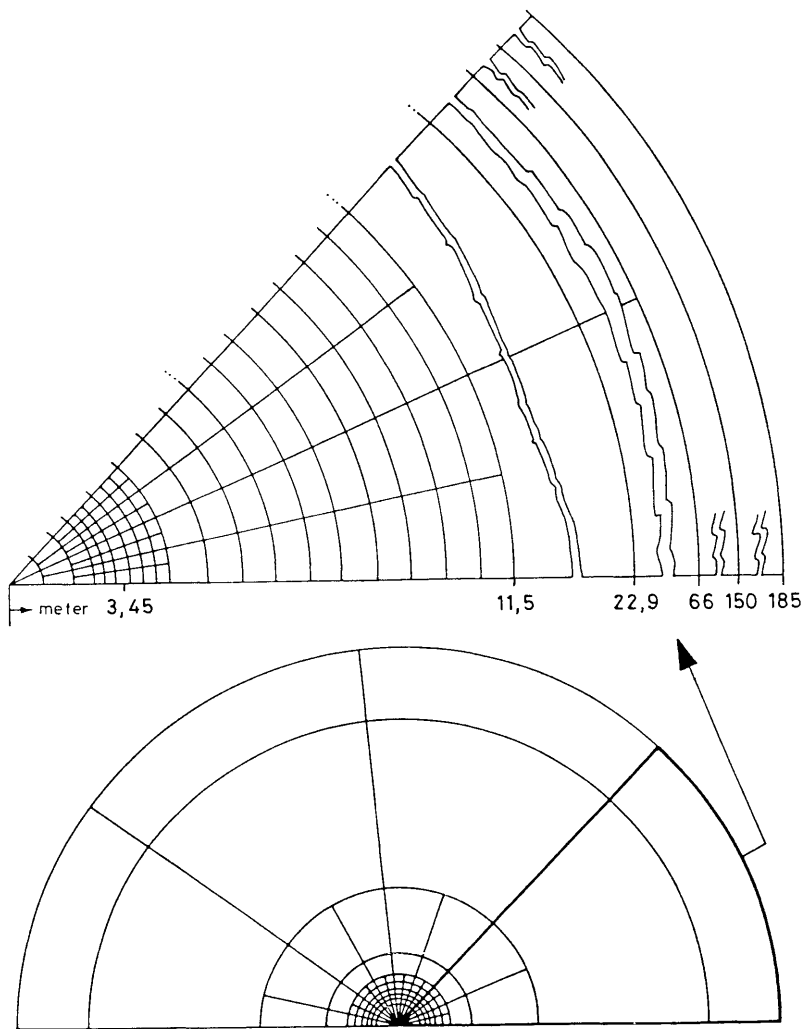


Figure 11 The network for "Lyuko" case

- Determine the practical possibility and reliability of the combination of rock freezing and drainage for the depressurization of reservoir layers.
- Determine the proper system of reservoir depressurization (if allowed).

After completing the freezing holes (knowing their actual location and inclination) an additional model study was requested by the Purchaser

- to determine the necessity and the proper location of additional freezing holes and
- to determine the proper location of temperatures test holes.

In the future, during the 8 freezing operations, more model studies will also be requested for model verification and for supporting the operative management, but the freezing has not started yet.

5.3 The construction of the model and the input data

Based on the experiences of the test case (see Table 2) two-dimensional modelling was decided upon with a more detailed and more extended network (see Figure 11).

For preliminary studies only half of the space was modelled. In the second phase of the study during modelling the actual location and inclination of the freezing holes bored before, two halves of the space were used for modelling the whole area with a reasonable number of nodes.

Two characteristic layers were composed representing the pessimistic parameters of each depth interval (0-125 m and 125-250 m).

The data of each layer and the data of the characteristic layers are given in Figure 10. The origin of the input data is also marked in Figure 10.

5.4 Some interesting results and consequences

It was only a routine task to determine that the total freezing capacity is enough to form the proper freezing mantle around the upper (0-125 m) interval during the planned three months period even under pessimistic conditions of hole inclinations, even in the streamside area (see Figure 12).

Having determined the necessary freezing capacity for maintaining the stationary status of the frozen mantle in the upper interval, the freezing process of the lower interval (the 2nd characteristic layer) was computed applying the remaining capacity of the freezing station (75%) under conditions of pessimistic inclination of holes.

Figure 13 presents the status of the frozen wall after a 5 month period of freezing. According to this computation the insufficiency of the freezing capacity appeared in the case of pessimistic location and direction of hole inclination.

Taking into account the limited capacity of the freezing plant and also the working capacity of the drilling rigs available, the necessity of additional measures (reservoir depressurization) also appeared.

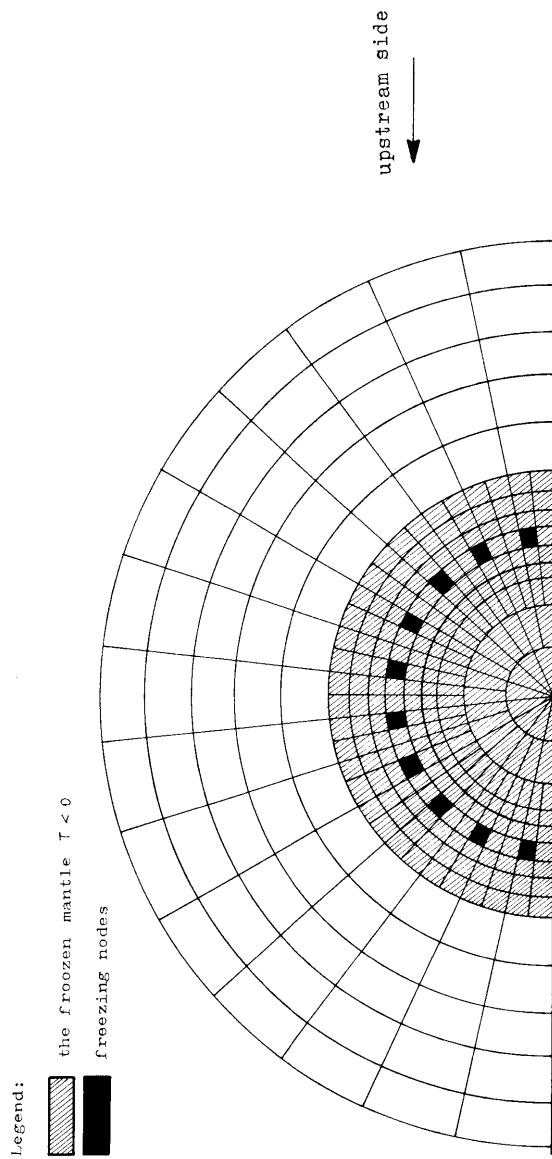


Figure 12 The frozen mantle at the depth of 120 m (1st standardized layer) after 3 months of freezing

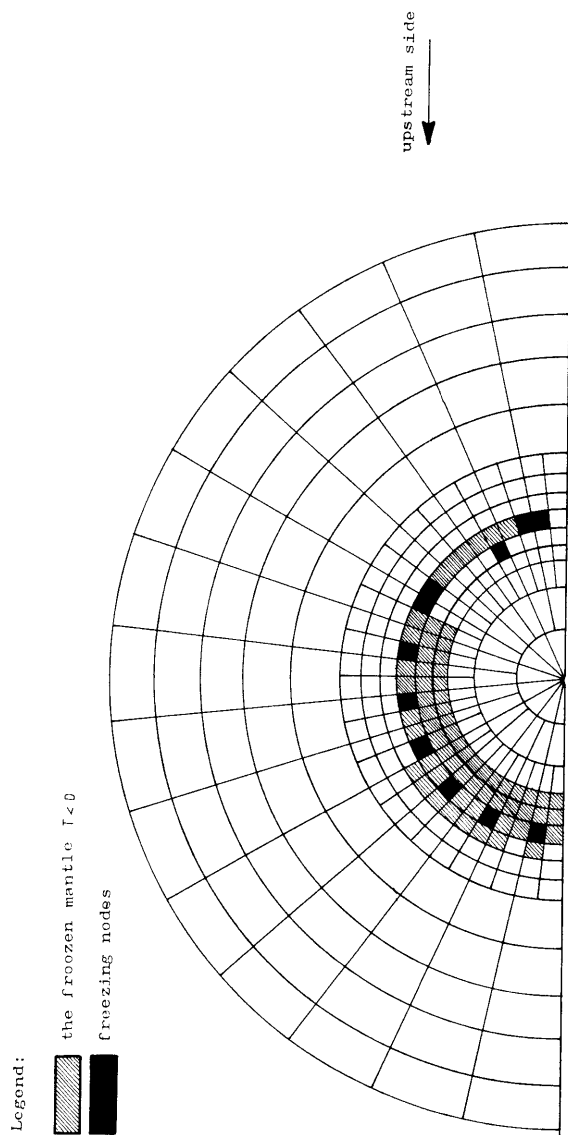


Figure 13 The status of the frozen mantle at the depth of 250 m (at the 2nd standardized layer) after 5 months of freezing, under conditions of pessimistic direction and location of the freezing holes

- More varieties of depressurization (water level lowering) were modelled, as listed below:
- Four filter-wells crossing the whole series of the layers, conducting the water by gravitation into a roadway were computed first in two versions:
 - (i) the wells start to operate after forming the frozen mantle,
 - (ii) the depressurization and freezing operate simultaneously.

Because of the differences of the working capacities of these wells, 2-4 m water-head differences between the individual well-nodes were modelled. According to Figure 14 these differences cause a strong flow rate, which "flushes out" the frozen mantle or destroys any freezing process (see Figure 13).

According to the computations presented above, the risk of the application of an improper, uncontrolled water level lowering exists during or after the freezing. The only kind of water level lowering that may be allowed, consists of wells of well known and controlled operating pressure. The system of wells should be properly located to form an inner field of seepage where the hydraulic gradient is not more than 0.1 m/m.

To fulfill these requirements, decisions were taken to implement separate well subsystems for each layer, and these wells should be bored from the mine and equipped with valves for controlling continuously the water head in the wells (see Figure 15 (a)). Figure 15 (b) presents the quasi-stationary seepage conditions inside the circle of a six-well system. This way of depressurization does not disturb the freezing process, but the consequence of an inflow through a window of the frozen mantle can easily be eliminated.

As a consequence of the computations presented above, a depressurization system according to Figure 15 (a) was decided upon by the Investor to increase the safety of sinking at the lower interval (180-250 m). According to the model studies the depressurization system must be put into operation two months prior to the freezing of the upper freezing interval.

For the upper interval no additional measures were decided because of the sufficiency of freezing and of difficulties of long holes to be bored from level -256.

Having completed all of the 19 freezing holes, inclinometer tests were carried out. Because of the strong inclination of many holes four additional holes were decided to be excluded from the freezing operation because of its extremely great inclination. Finally, these 19-4=15 holes were put into the model with their actual location and inclination (see Figure 15 and 16).

As presented in Figure 16 the inclinations of holes do not disturb the freezing process in the upper interval. But for the lower interval additional freezing holes are necessary (see Figure 17).

Although a modest seepage rate ($v = 0.5$ m/day) was taken into account, the convective heat transport strongly modified the forming of the freezing mantle as well as the necessity and the location of additional holes (see Figure 16).

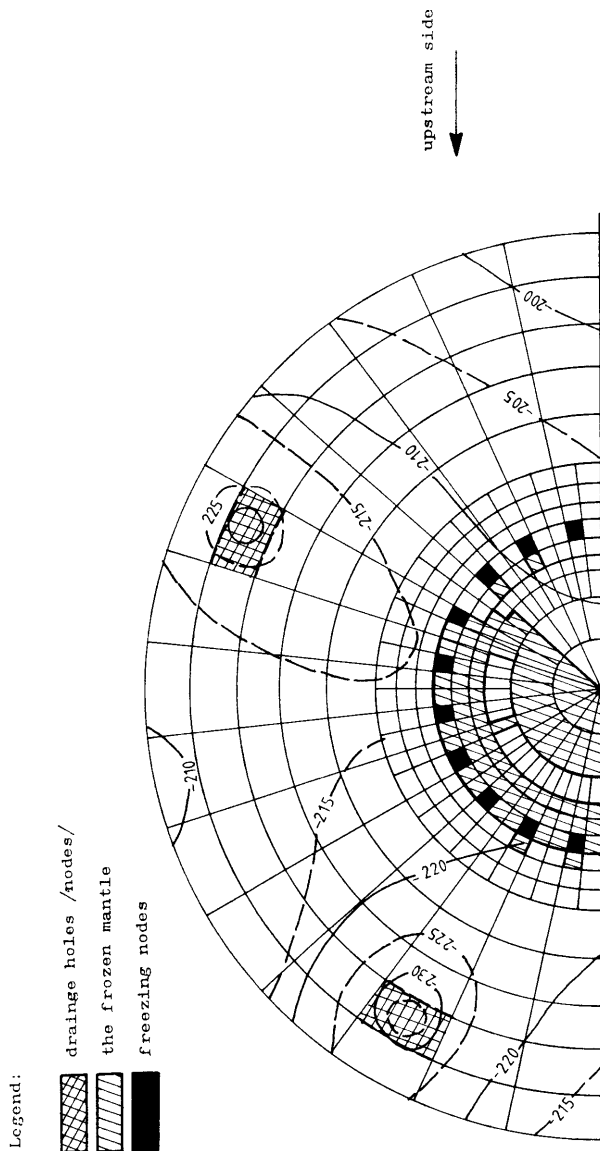



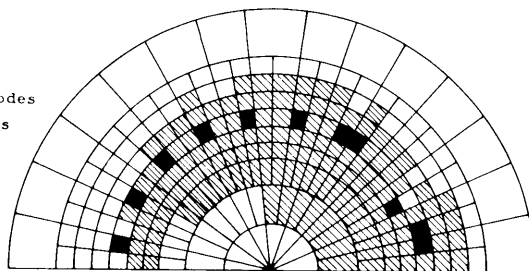


Figure 14 The frozen mantle and the isohypses of water seepage in case of applying water level lowering/with four wells / simultaneously with freezing

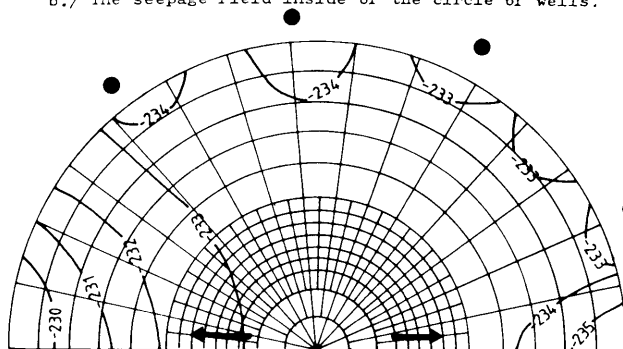
a./ The frozen mantle after 5 month

Legend:

-  the frozen nodes
-  freezing nodes
-  drainage holes



b./ The seepage field inside of the circle of wells.



c./ The location of the wells

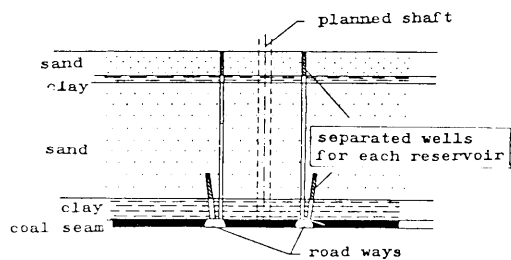





Figure 15. A quasi-acceptable depressurization-system with 8 wells for combining with rock freezing

Legend

-  $T = 0^{\circ}\text{C}$
-  Freezing node /element/ in the model
-  $T < 0$ the frozen mantle

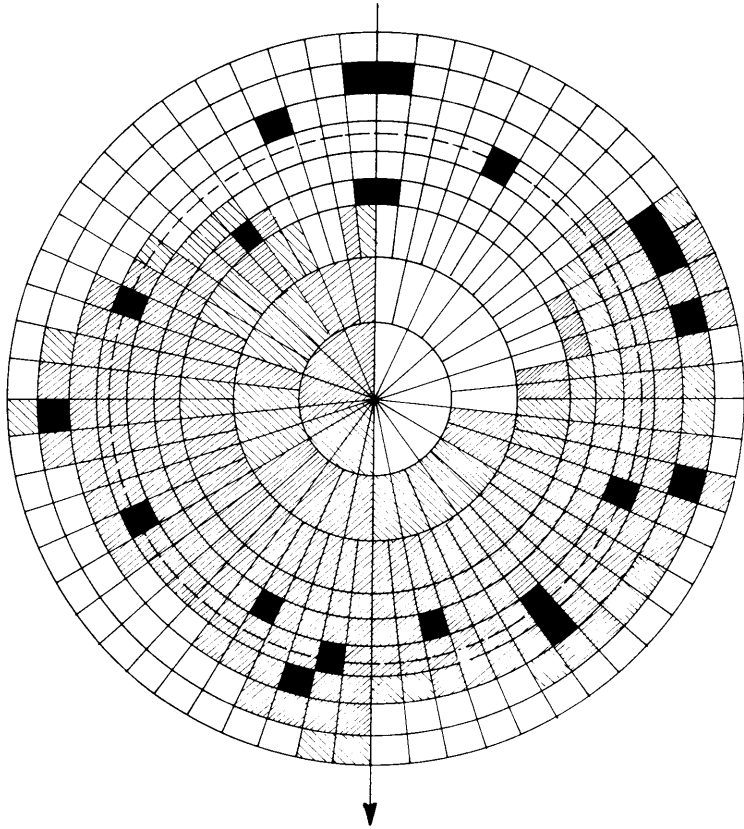





Figure 16 The isotherms and the frozen mantle at depth of 120 m (at the 1st standardized layer) after 11 weeks of freezing (with full capacity, freezing fluid temperature -23°C) using the actual (measured) data on borehole inclinations

Legend

-  the frozen mantle
-  $T = 0^{\circ}\text{C}$
-  freezing nodes

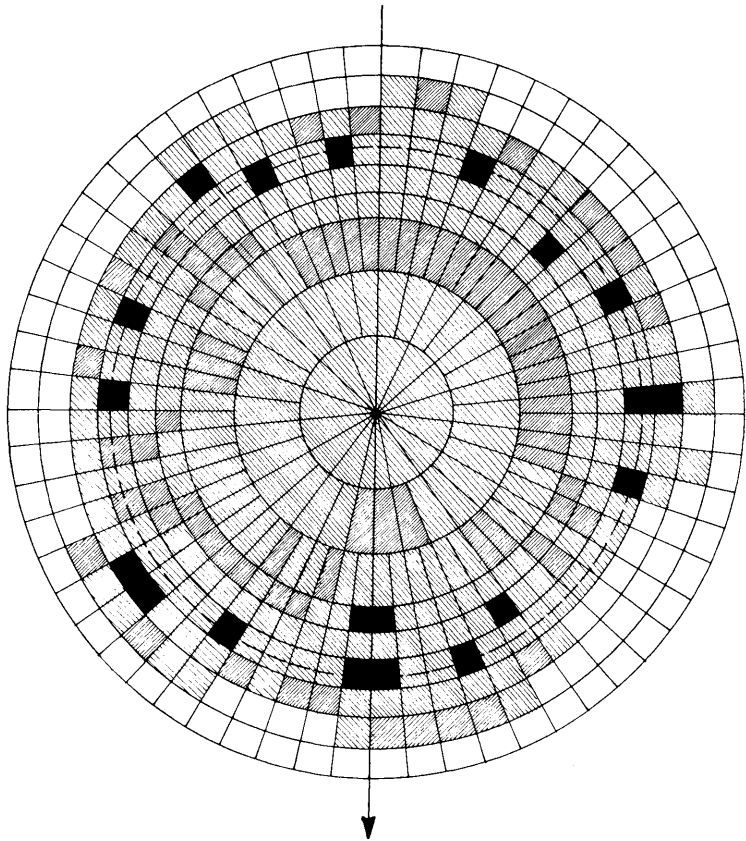


Figure 17 The frozen mantle at depth of 250 m, at the 2nd standardised layer, 20 weeks of freezing, fluid temperature -23°C , using actual (measured) data of borehole inclinations

As a consequence of this computation, it was decided to drill four additional freezing holes.

6. FINAL CONCLUSIONS

The new model of rock freezing and water seepage has demonstrated its potentiality to simulate even the most sophisticated cases, which occurred or may occur in the rock freezing practice.

The model offers new possibilities to apply new combinations (eg rock freezing and water depressurization).

Although the model is a sophisticated one, it was adopted to professional personal computers (eg IBM AT) which are used widely even by the contractor firms.

For these reasons the model can be used successfully to support the design and the operative management of freezing operations even under impact of water seepage and of its combination with other processes (eg water level lowering and grouting).

The application of the model cuts costs and decreases the risk of failures.

ACKNOWLEDGEMENTS

The paper is based on a research project No 220.002.0 financed by the Ministry of Industry in Hungary and on a design project No 237.002.6 financed by Borsod Coal Mines. The authors express their thanks to the Borsod Coal Mines and to the Central Institute for Mining Development, Hungary for the permission of publication and to the Hungarian Shaft Sinking Enterprise for providing many data and for their kind and useful cooperation.

We should like to express our personal thanks to Mr. J. Honvéd Min.E. Dept. Head and Mrs. K. Puch Hydrog.E., Mr. G. Máthé (Shaft Sinking Ent.) for providing data and advice, and to Mr. G. Reményi Min.E. Chief Eng. of Development and Mr. A. Szepessy Hydr.E. Head of Mine Water Control for providing the best possibility to put the new method into practice.

REFERENCES

Belferman, M U, Designing the best technology of rock freezing for protecting shaft sinking operations (Shahtnoe Stroitelstvo No 7 1982. p 6-8 in Russian)

Hegelman, J, Konzept und Stand der Arbeiten am tiefen Gefriershaf Voerde (Gluckauf No 118. T.2 1982. p 76-81)

Honvéd, J, Shaft sinking using special methods (Manuscript in Hungarian) Hungarian Shaft Sinking Enterprise, 1986

Del Guidence; Comini G, Finite elements simulation of freezing process in Soils. Int Journ for Numerical and Analytical Methods in Geomechanics. 1978

Sabela, R, Modeluntersuchungen zur Frostbreitund im Gefrierschachtbau Gluckauf Forschungshefte 43. (1982) H 3 p 94-99

Seleznev, N.A, Sedin, S.A Experiences on combination of rock freezing and water level lowering at Belozorsk iron ore mine (Shahtnoe Stroitelstvo 1982, 2 p 29-30)

Ries, A, Geschichtliche und technische Entwicklung des Gefriersverfahrens im Schachtausbau Gluckauf 118. (1982) No 2 p 65-75

Wild, W.M, Forrest, W, The application of the freezing process of ten shafts and two drifts at Selby project. The Mining Engineer 1984, No 229, Vol 139, p 713-721